SLAC-PUB-2260
February 1979
(I)

MODEL FOR FLUX TRAPPING AND SHIELDING BY TUBULAR SUPERCONDUCTING SAMPLES IN TRANSVERSE FIELDS*

David J. Frankel

Stanford Linear Accelerator Center
Stanford University, Stanford, California 94305

ABSTRACT

Experiments have been carried out on the flux trapping and shielding capabilities of tubular superconductors in transverse dipole and quadrupole fields. Field profile measurements are reported for tubes of vapor-deposited Nb_3Sn and samples assembled from spirally wound strips of Nb-Ti/Cu sheet composite. The flux trapping and shielding process is modeled by assuming that critical state currents flow in saddle-shaped paths in the sample walls. Good correspondence between the experimental and model-generated field profiles is achieved. The model can be used in the design or analysis of flux trapping and shielding devices, or to obtain estimates of the average critical current density from measurements of the trapping or shielding ability of tubular samples.

(Submitted to IEEE Trans. Magn.)

*Supported by the Department of Energy, Contract No. EY-76-C-03-0515.

INTRODUCTION

It has been shown that tubular superconducting samples can be used to effectively trap and shield fairly large and complex transverse multipole magnetic fields [1, 2, 3, 4, 5, 6, 7]. On a microscopic scale, trapping and shielding of flux is explained by the pinning of the magnetic flux lines in local free energy minima created by inhomogeneities in the superconducting material. On a macroscopic scale, the flux trapping and shielding can be viewed as arising from the action of induced trapping or shielding currents. The level of these currents can be related to the pinning forces by assuming that the forces pinning a flux line in place just balance the driving forces on it. Materials in the critical state [8] are assumed to respond to changes in the magnetic field with induced currents that flow at the critical level defined by this force balance. Previously the macroscopic behavior of superconducting tubes, cylinders, and slabs in parallel fields [8, 9, 10], and of disks in axial fields [11], has been accounted for by using critical state models. In this paper such a model is applied to the problem of the magnetic behavior of tubular superconductors in transverse fields. Since the equations which determine the actual form of the induced current pattern for this geometry are quite complicated, an approximate form for the critical state current pattern was used.

CRITICAL CURRENT MODEL

The response of the superconductor to an applied transverse field was modeled by assuming that the critical currents flow axially down the sides of the tubular samples and follow circular arcs across their ends (Fig. 1). An expression for the transverse field at a point along the axis a distance ℓ_1 from one end and a distance ℓ_2 from the other end of a pair of circular-head coils can be derived from the Biot-Savart Law [12]. The result is:

$$B_x = \frac{\mu_0 I}{\pi R}\left[\frac{c(2+c^2)}{(1+c^2)^{3/2}} + \frac{d(2+d^2)}{(1+d^2)^{3/2}}\right]\sin\phi \qquad (1)$$

where, as shown in Fig. 1,

$c = \ell_1/R \qquad d = \ell_2/R$

$L = \ell_1 + \ell_2 =$ length of the straight segments

$R =$ radius of the curved end segments

$2\phi =$ angle included by a curved end segment.

The field generated by the critical currents in the sample was computed by summing field contributions from a series of such pairs of circular-head coils arrayed on the sample surface. The number of pairs of current paths, N, was typically between 15 and 31. The current per path was set equal to the product of an assumed current density and the cross-sectional area of the current paths:

$$I = J_c \Delta s \Delta r .$$

Thin-walled samples were modeled by setting the effective thickness of the current paths, Δr, equal to the thickness of the sample wall, while thick-walled samples were modeled by adding contributions from a series of current sheets located at decreasing values of the radius. The effective width of the straight sections, Δs, was equal to $\pi R/2N$. The width of the circular sections, ΔL, was between $\pi R/2N$ and $0.5L/(N-1)$. A width of $\pi R/2N$ for the circular segments resulted in a uniform current density on the sample surface and a current pattern (for $2\pi R < L$) in which the straight sections of the current paths reached the center of the surface before the circular sections. Choosing $\Delta L = 0.5L(N-1)$ resulted in lower current density in the circular-end segments than along the straight sections, and a current pattern in which all the current paths reached the center of the tube surface at once. This pattern resulted in profiles with steadily increasing values of B_x towards the center of the tube, while the uniform current density pattern resulted in steeper field gradients near the ends of the tube and a flatter profile near its center. The presence of an applied field was simulated by adding a uniform field of the appropriate polarity to the field generated by the circulating currents. The relation between the critical current and the field was limited to the simple form J_c = constant, since field values were calculated along the axis of the tube, and not in the sample wall.

The field due to currents flowing over a limited portion of the sample surface was calculated by restricting the values of ϕ to between $\pi/2$ and some angle greater than zero. However, the field profiles along the axis of the tube were insensitive to such changes as long as the total circulating current was kept constant. It was also possible to vary the current density with angular position in a given manner. A current distribution, $J = J_0 \sin\phi$, expected to generate a roughly uniform transverse field inside the tube, produced $B_x(z)$ curves with a form similar to ones generated with $J(\phi)$ = constant, but with approximately half the peak field intensity.

A variation of the current model was applied to the problem of analyzing the trapping of transverse quadrupole fields. An ideal 2-dimensional quadrupole field is generated in the interior of a long tubular conductor by a cylindrical current distribution described by [13] :

$$\sigma(\phi) = \frac{2}{\mu_0} G r \cos(2\phi) , \qquad (2)$$

where σ is the linear current density (A/m) flowing in the axial direction on a cylindrical surface of radius r, G is the gradient of the quadrupole field generated by the currents, and ϕ is the azimuthal angle. If end effects are neglected, this equation can be used to estimate the current densities required to trap quadrupole fields.

EXPERIMENT

The experimental apparatus and procedures were similar to those described in [11]. Tubular samples suspended within the dewar from a long, thin-walled stainless steel tube were oriented so that a uniform magnetic field could be applied perpendicularly to the sample axis. The field was measured by Hall effect probes [14] mounted in a cylindrical epoxy-fiberglass holder which could be translated along the axis of the hollow samples, or rotated around their inner peripheries. The position of the probe holder was monitored by a potentiometer coupled to a driving mechanism located on top of the dewar. Flux trapping experiments were carried out by establishing a magnetic field in the sample while its temperature was above T_c, cooling the sample to 4. 2 K (or below) while the applied field remained constant, and then reducing the applied field to zero. Shielding experiments were performed by cooling the sample in zero field and then gradually applying a field. The steady increase or decrease of the applied field was periodically halted and a field profile obtained by translating or rotating the Hall probe holder. This procedure generated curves of the transverse component of the field inside the tubular samples as a function of axial or azimuthal position, at a series of values of the applied field (solid curves in Figs. 2, 3, 4, and 5).

RESULTS

Nb_3Sn Samples

The Nb_3Sn samples [15, 16] consisted of alternate layers of Nb_3Sn and Nb-Sn alloy, or Nb_3Sn and yttrium, vapor-deposited onto 6. 4 mm diameter, 75. 6 mm long Hastelloy tubes. Total thickness of the Nb_3Sn in these layered samples was 6-7 microns. Uniform fields of approximately 0.12-0.16 T could generally be trapped or shielded by the tubes, and differences of more than 0.20 T between the fields inside the tubular samples and the applied fields were observed in some cases. Flux jumping limited flux trapping ability at low fields, while at higher fields, typically above 0.30-0.60 T, flux jumping ceased to occur.

The trapping and shielding process in these samples was simulated with the model described above. The model adequately described the shape of typical trapping and shielding profiles, and gave critical current values of up to $3-4 \times 10^{10}$ A/m^2, in agreement with values measured in axial fields by Howard. The model also indicated that most flux jumps took place at field differences of roughly 50-100% of the maximum possible for the thickness and critical current density of the material. Figure 2 shows typical field profiles obtained during a flux trapping test of the Nb_3Sn sample tube 75-94, along with profiles generated with the model. This tube consisted of alternate layers of 0.4 microns of Nb_3Sn and 0.009 microns of yttrium, with a total thickness of the Nb_3Sn of 6.9 microns. Howard measured a T_c of 16.4-17.5 K and a zero field critical current at 4.2 K of 4.2×10^{10} A/m^2 for this sample. In the test shown, the sample was cooled in a uniform transverse field of 0.115 T, and scans of the transverse field along the sample axis were taken at five intermediate field levels as the applied field was reduced to zero. A partial flux jump occurring between $B_a = 0.016$ T and $B_a = 0$ resulted in the loss of some trapped flux from part of the tube. The model-generated curves were calculated by assuming that a uniform current density at the levels indicated in the figure flowed in the Nb_3Sn coating. A nearly identical set of model curves was generated by holding J_c fixed and varying the angle ϕ, which determines the fraction of the sample carrying critical state currents. Similar behavior and agreement between the model and experimental trapping and shielding curves were obtained with the other Nb_3Sn tubes.

Nb-Ti Samples

A composite material containing Nb-55wt%Ti and copper in the form of a sandwich of three layers of Cu interleaved with two layers of Nb-Ti was fabricated by roll-reducing the sandwich to a thickness of 0.25 mm [17]. The composite was heat-treated in vacuo at a temperature of 355°C for periods of up to 130h to improve pinning and critical currents. Tubular samples were assembled from one or more strips of the sheet composite by winding the strips into spirals on a copper tube. The inner ends of the strips were soldered to the copper tube, and the strips were held in place either by fitting a larger copper tube snugly over the spirals, or by tightly winding stainless steel wire around the spirals.

Figure 3 shows field profiles obtained during a trapping test of a sample assembly consisting of a 54.4 mm wide by ~ 250 mm long Nb-Ti/Cu strip wound into a 3-layer spiral on a 23.2 mm diameter copper tube. This strip had been heat-treated for 48 h at 355°C. In the example shown, the close correspondence between the model-generated and measured field profiles was obtained by assuming a current density of 2.55×10^9 A/m^2 in the Nb-Ti layers, and setting ΔL equal to $0.5L/(n-1)$. Model calculations of field profiles for a number of similar sample assemblies of varying diameters and lengths were generally in good agreement with experimental curves. Exact correspondence could not always be obtained for the samples with the highest flux trapping and shielding capabilities because the effect of the dependence of the critical current on field level was not included in the model.

Several strips 43 - 45 mm wide by ~300 mm long were used to investigate the feasibility of building up a long sample tube from shorter spirals. The strips were heat-treated for 24 h at 350 °C in order to obtain a combination of moderate current densities ($1-2 \times 10^9$ A/m^2) and good stability against flux jumping. Pairs of strips were placed end to end, and were wound into 4-layer spirals on a 45.7 mm diameter copper tube. Figure 4 shows typical trapping and shielding profiles obtained with a sample assembly in which two 4-layer spirals were placed side by side. In this arrangement the spirals act nearly independently, and the field easily penetrates through the small gap between the spirals. The dashed curves in the figure were generated by superimposing the calculated shielding or trapping effect of the two adjacent subassemblies. The correspondence between the model and experimental curves is quite good, although the field penetration near the gap between the spirals was somewhat greater in practice than indicated by the model calculation. Figure 5 shows curves obtained with two spiral subassemblies overlapping by 3.2 mm. The field penetration is slightly reduced in this case. The calculated curves (dashed lines in Fig. 5) show a corresponding decrease in field penetration, although the measured effect is still larger than that indicated by the model calculation. Even with the overlap, the assembly acts as two nearly independent spirals rather than one long tube. The field penetrates through any available opening or break in the superconductor, and as a result the shielding currents in each section of the assembly flow in the manner required to shield the field from that section. Therefore, when building up a large device from smaller subsections, sufficient overlap must be provided to attenuate the field penetrating through the breaks in the superconductor. The current model described here can be used to model the effect such breaks will have on the performance of the device.

Quadrupole Fields

Several samples, including a hollow lead cylinder and two hollow niobium cylinders, have been tested in quadrupole fields [2, 3]. The simple current model was able to account for the trapping capabilities of these samples. Current levels predicted by (2) on the basis of the maximum quadrupole fields trapped agreed well with estimates of critical currents based on dipole field measurements and the current model based on (1).

CONCLUSIONS

The use of saddle-shaped paths for the critical state currents in the tubular samples resulted in good correspondence between experimental and model-generated field profiles. However, since the shapes of profiles along the sample axis were insensitive to some of the details of the current distribution, it was not possible to completely define the pattern for the critical state currents. The model was also limited to the simple approximation $J_c(B) \approx$ constant since only the field along the axis and not the field near the superconducting material was calculated. However, this approximation fails only when there is a large variation in the field in the sample, or when J_c varies rapidly with changes in field. Even in these cases the model can be used to obtain estimates of flux trapping or shielding abilities by using a J_c appropriate to the average field in the sample wall. The model described here can be used to aid in the design and analysis of devices used for trapping dipole, quadrupole, and higher order multipole fields, and devices that are built up from a number of subassemblies. In addition, if the critical currents are not known the model can be used to obtain estimates of the average critical current in tubular samples from measurements of their trapping or shielding abilities. The model should prove to be useful in developing practical flux trapping and shielding devices for use in high energy physics applications.

REFERENCES

[1] F. Martin, S. J. St. Lorant, and W. T. Toner, "A four-meter long superconducting magnetic flux exclusion tube for particle physics experiments," Nucl. Instrum. Methods, vol. 103, pp. 503-514, August/September 1972.

[2] M. Rabinowitz, E. L. Garwin, and D. J. Frankel, "An investigation of the very incomplete Meissner effect," Nuovo Cimento Lett., vol. 7, no. 1, pp. 1-4, 5 May 1973.

[3] E. L. Garwin, M. Rabinowitz, and D. J. Frankel, "Permanent multipole magnetic fields stored in superconductors," Appl. Phys. Lett., vol. 22, no. 11, pp. 599-600, 1 June 1973.

[4] D. J. Frankel and E. L. Garwin, "Field replication and flux shielding in annular superconductors," IEEE Trans. Magn., vol. MAG-13, no. 1, pp. 205-208, January 1977.

[5] D. J. Frankel, "Flux trapping and shielding in irreversible superconductors," Ph.D. Dissertation, Stanford University, June 1978. (Also available as Stanford Linear Accelerator Center Report SLAC-211.)

[6] M. Rabinowitz, H. W. Arrowsmith, and S. D. Dahlgren, "Dependence of maximum trappable field on superconducting Nb_3Sn cylinder wall thickness," Appl. Phys. Lett., vol. 30, no. 11, pp. 607-609, 1 June 1977.

[7] E. U. Haebel and W. Witzeling, "A superconducting multi-ribbon shielding tube," 6th Int. Conf. on Magnet Tech., Bratislava, Czechoslovakia, 29 August - 2 September 1977, Vol. 2. Bratislava: Alfa, 1978, pp. 949-954.

[8] C. P. Bean, "Magnetization of hard superconductors," Phys. Rev. Lett., vol. 8, no. 6, pp. 250-253, 15 March 1962.

[9] Y. B. Kim, C. F. Hempstead, and A. R. Strnad, "Magnetization and critical supercurrents," Phys. Rev., vol. 129, no. 2, pp. 528-535, 15 January 1963.

[10] W. A. Fietz, M. R. Beasley, J. Silcox, and W. W. Webb, "Magnetization of superconducting Nb-25%Zr wire," Phys. Rev., vol. 136, no. 2A, pp. A335-A345, 19 October 1964.

[11] D. J. Frankel, "Critical state model for the determination of critical currents in disk-shaped superconductors," to be published in J. Appl. Phys.

[12] F. K. Harris, "Coil arrangements for producing a uniform magnetic field," Research Paper RP716, J. Res. Natl. Bur. Stand. (U.S.), vol. 13, pp. 391-410, September 1934.

[13] R. A. Beth, "Fields produced by cylindrical current arrays," Brookhaven National Laboratory Report No. AADD-102, March 1966.

[14] Bell FH-301-040, F. W. Bell Inc., Columbus, Ohio.

[15] R. E. Howard, "Low field critical currents and ac losses of thin film niobium-tin superconductors," Ph. D. Dissertation, Stanford University, 1976.

[16] R. E. Howard, C. N. King, R. H. Norton, R. B. Zubeck, T. W. Barbee, and R. H. Hammond, "Critical current and ac loss of coevaporated Nb_3Sn superconductors," Advan. Cryog. Eng., vol. 22, pp. 332-340, 1977.

[17] Teledyne - Wah Chang Albany, Albany, Oregon.

FIGURE CAPTIONS

1. Critical current model for tubular samples in transverse fields. Lower portion of the figure shows field distribution obtained when a series of current loops cover the surface of the tube.

2. Field profiles along the axis of sample 75-94 obtained during a flux trapping test (solid curves) together with corresponding model profiles calculated with $J_c = 0.42 \times 10^{10}$ (●), 0.83×10^{10} (×), 1.15×10^{10} (O), 1.53×10^{10} (▲), and 1.80×10^{10} A/m^2 (□).

3. Field profiles obtained during a flux trapping test of a Nb-Ti/Cu 3-layer spiral assembly. In this case the sample was initially cooled in a 0.7T field. Dashed curve was generated by the model using $J_c = 2.55 \times 10^9$ A/m^2.

4. Flux trapping (a) and shielding (b) profiles obtained with two Nb-Ti/Cu spiral assemblies butted together.

5. Flux trapping (a) and shielding (b) profiles obtained with two Nb-Ti/Cu spiral assemblies overlapped by 3.2mm (shaded region).

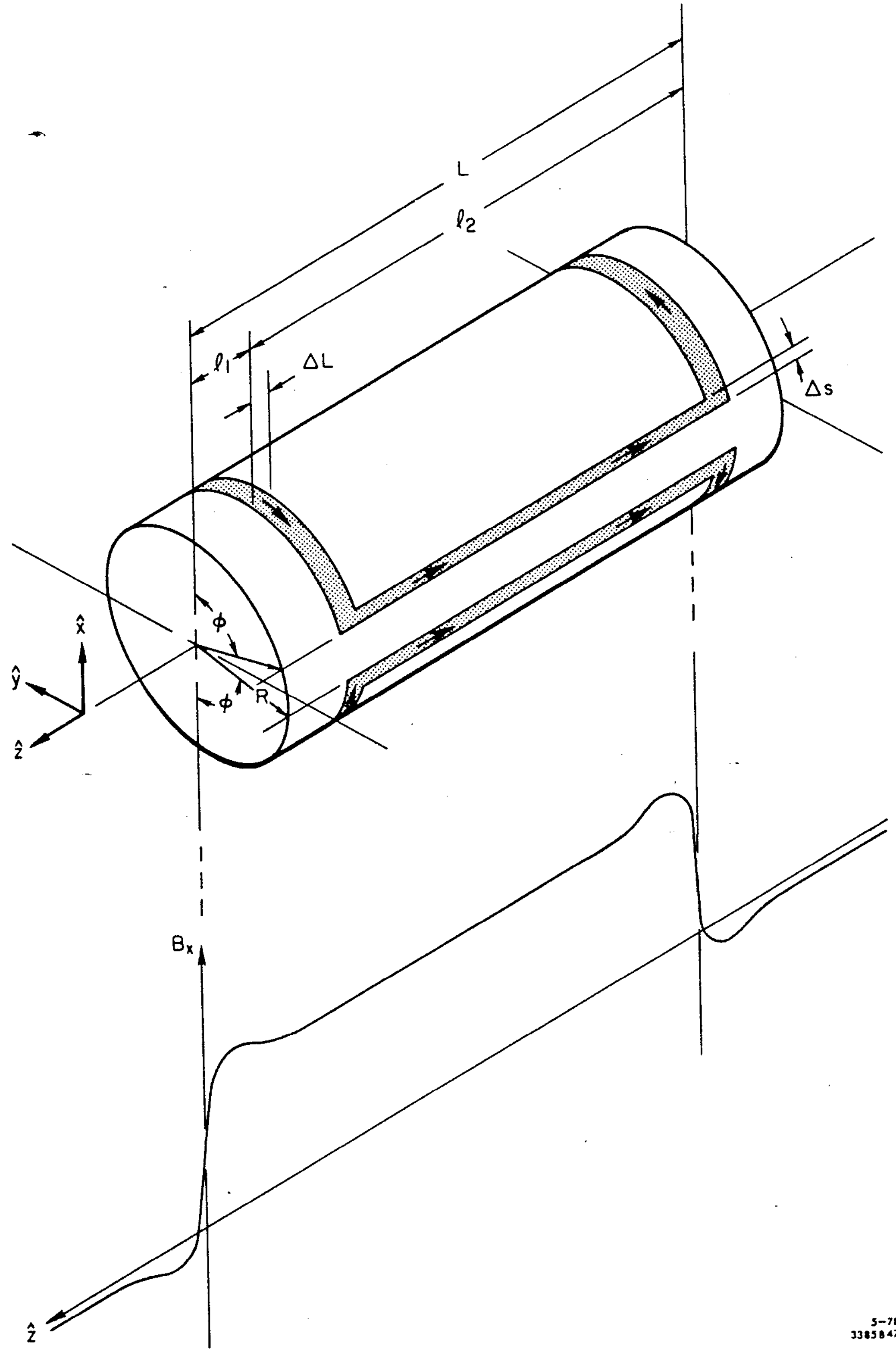

Fig. 1

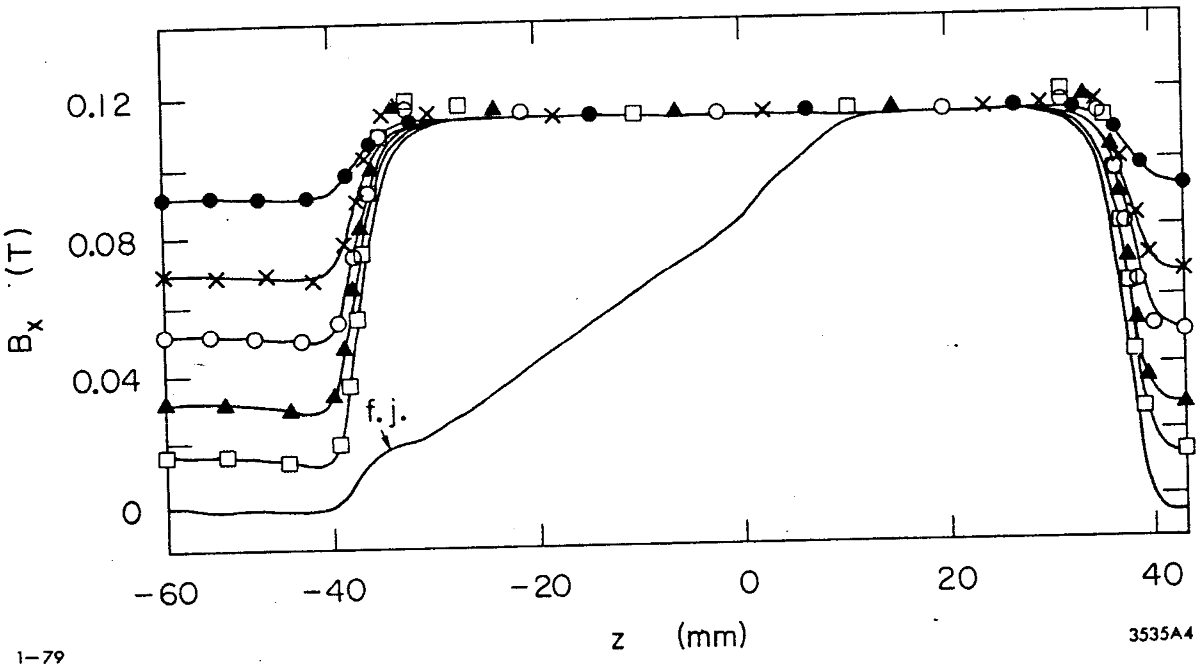

Fig. 2

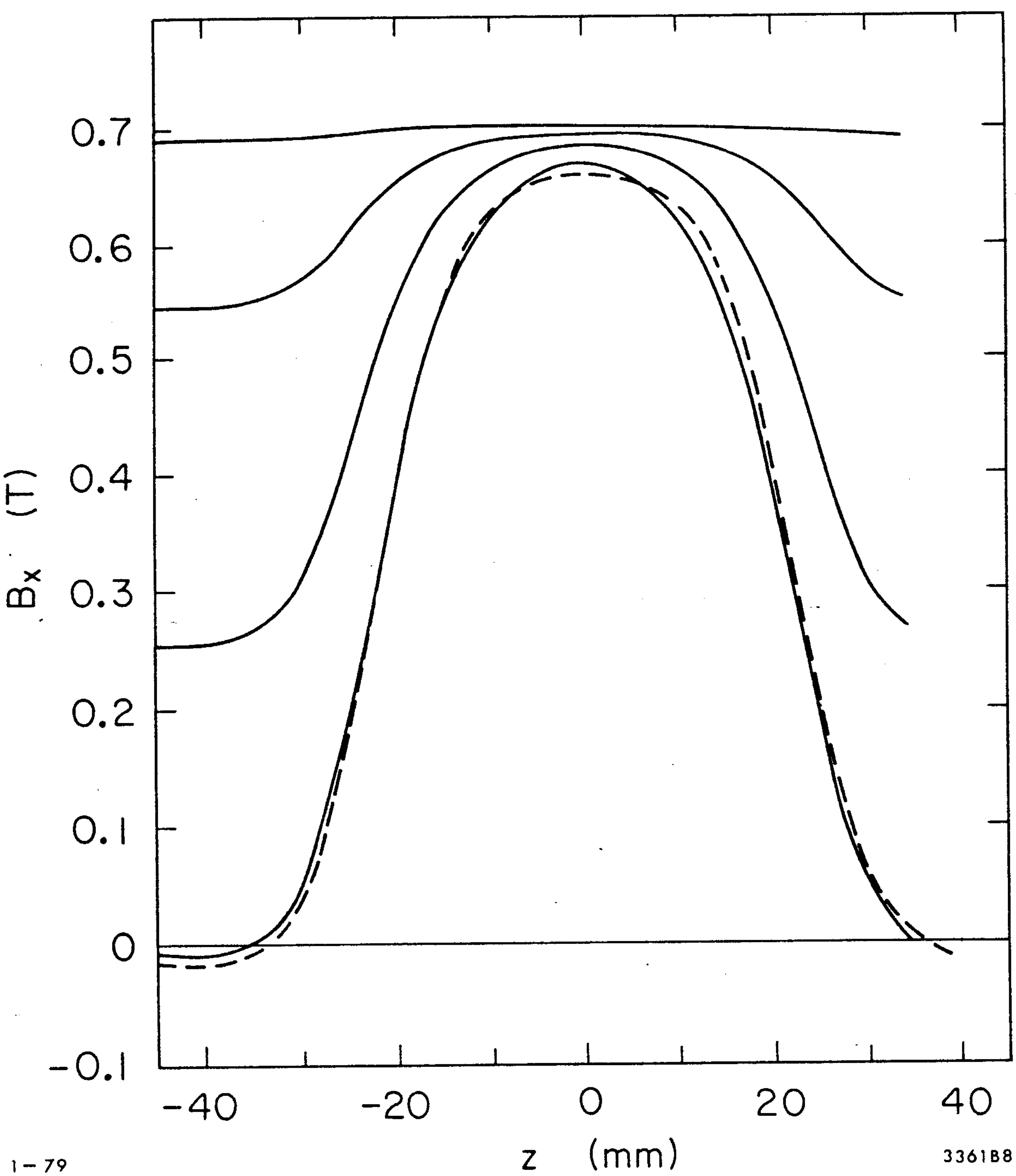

Fig. 3

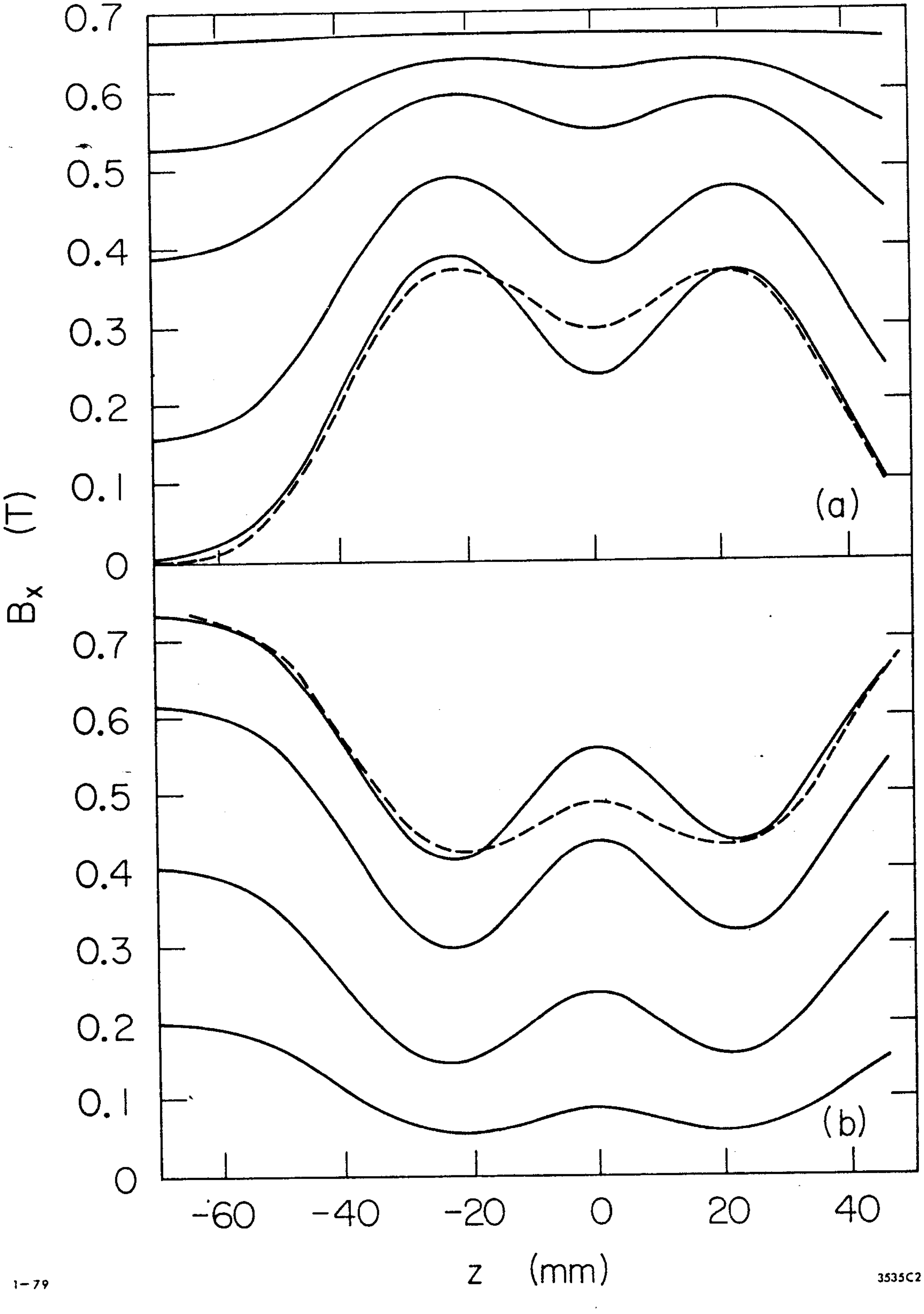

0.7
0.6
0.5
0.4
0.3
0.2
0.1
0
B_x (T)
(a)
0.7
0.6
0.5
0.4
0.3
0.2
0.1
0
(b)
-60
-40
-20
0
20
40
z (mm)
1-79
3535C2

Fig. 4

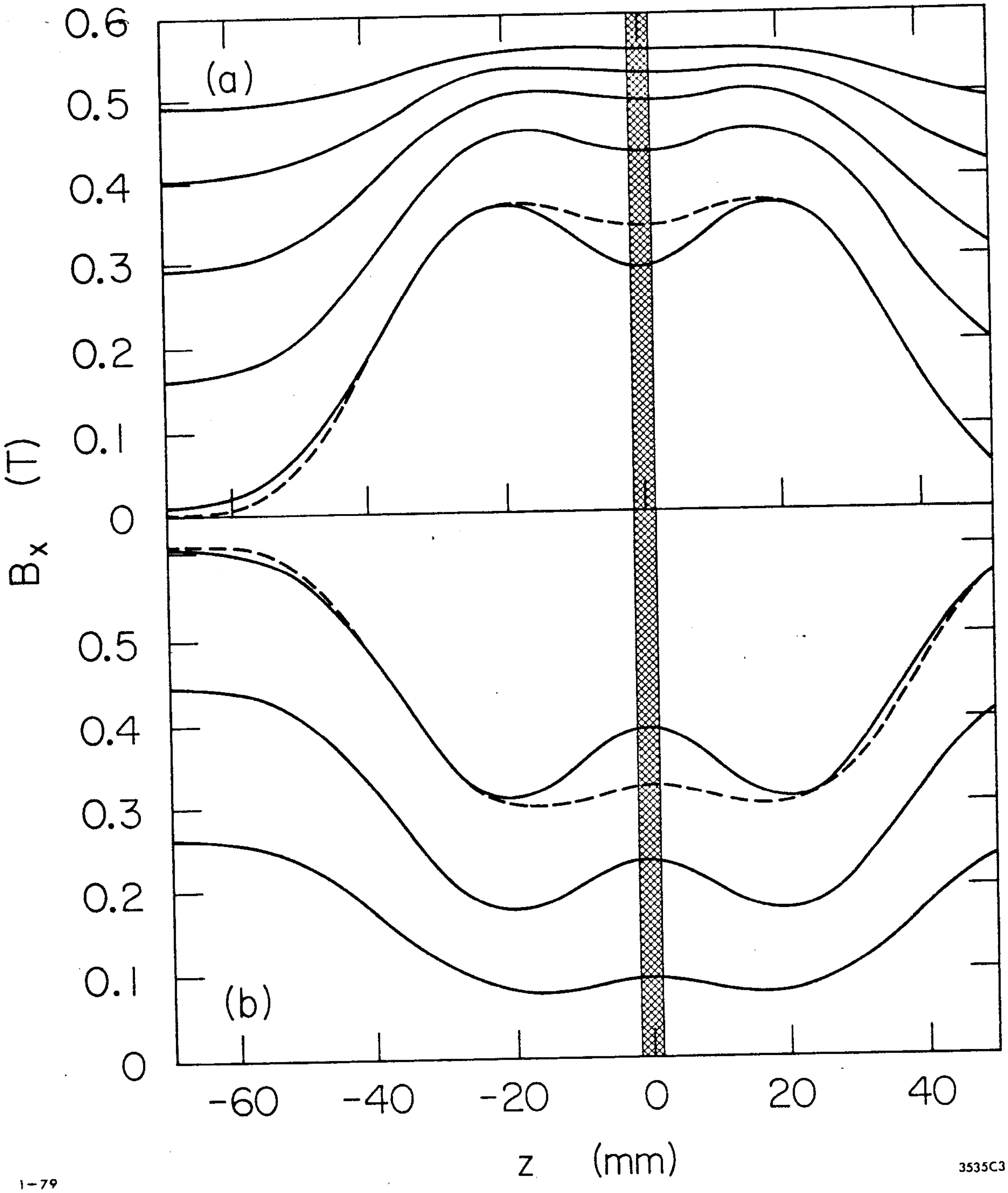

0.6
0.5
0.4
0.3
0.2
0.1
0
(a)
0.5
0.4
0.3
0.2
0.1
0
(b)
B_x (T)
-60
-40
-20
0
20
40
z (mm)
1-79
3535C3

Fig. 5